Controlling dissociative adsorption for effective growth of carbon nanotubes

Vijaya Kayastha and Yoke Khin Yap[a)]
Department of Physics, Michigan Technological University, Houghton, Michigan 49931

Svetlana Dimovski and Yury Gogotsi
Department of Materials Science and Engineering and A. J. Drexel Nanotechnology Institute, Drexel University, Philadelphia, Pennsylvania 19104

(Received 21 May 2004; accepted 17 August 2004)

Dissociative adsorption has been widely simplified as part of the vapor–liquid–solid (VLS) growth model. We found that the addition of specific carrier gases can critically modify the growth rate and growth density of multiwall carbon nanotubes (MWNTs). These results were explained by dissociative adsorption of C_2H_2 molecules and a solid-core VLS growth model. Based on these integrated mechanisms, vertically aligned MWNTs were grown with an initial growth rate as high as ~800 μm/h. This efficient growth process results at temperature and C_2H_2 partial pressures at which the decomposition and segregation rates of carbon are balanced. Appropriate use of carrier gas is one of the factors that could facilitate efficient and continuous growth of carbon nanotubes in the future. © *2004 American Institute of Physics*. [DOI: 10.1063/1.1806558]

Carbon nanotubes (CNTs)[1,2] are among the promising materials for applications in future nanoscale science and technology. For the synthesis of CNTs, thermal chemical vapor deposition (CVD) is a convenient technique for growing both single wall, and multiwall CNTs. The well-accepted growth mechanism of CNTs by thermal CVD involves the decomposition of hydrocarbon gases on the surface of catalyst, the diffusion of carbon into the catalyst until saturation, and subsequent segregation of carbon from the catalyst as a tubular structure. These processes are described as the vapor-liquid-solid (VLS) growth model.[3,4] In fact, the catalytic decomposition process is known as dissociative adsorption[5–7] and has been widely simplified in the VLS model. Ideally, CNTs will continue to grow if every carbon atom that deposits on the catalyst's surface becomes incorporated within the CNTs structure. Such an ideal condition has not been achieved due to the lack of understanding of the relations between the growth parameters and the decomposition, diffusion, and segregation processes. This is the main obstacle for continued growth of CNTs to unlimited tube lengths. The phenomena responsible for growth saturation and growth inhibition are not fully elucidated and just started to gain attention.[8,9]

Here, we found that the addition of carrier gas can convert a saturated growth of multiwall carbon nanotubes (MWNTs) into a continuous mode. We can grow MWNTs by pure C_2H_2 without the use of NH_3 for pretreatment and growth. This enables a systematic study on the function of carrier gases during the growth of MWNTs. Some previous reports indicated that ammonia (NH_3) gas is needed for the formation of the catalyst nanoparticles and the growth of the nanotubes.[10,11] We found that the addition of specific carrier gas can critically change the growth rate, and the growth density of MWNTs. We explain these results by dissociative adsorption of C_2H_2 molecules on iron (Fe) nanoparticles and the VLS growth model. Our result implies for an *in situ* technique that could control the decomposition rate of C_2H_2 on Fe, and the growth rate of MWNTs. The addition of appropriate carrier gas is one of the factors that could facilitate continuous growth of carbon nanotubes in the future.

The catalytic Fe films used in our experiments were coated on SiO_2/Si substrates in a pulsed-laser deposition system.[12,13] We used the fourth-harmonic generation of Nd:YAG laser (wavelength, $\lambda \sim 266$ nm) at an energy density of ~1 J cm^{-2} on the Fe target. Depositions were carried out at room temperature in a vacuum. These films had a thickness of 4 nm as verified by atomic force microscopy (AFM). For the growth of the MWNTs, these $Fe/SiO_2/Si$ substrates were inserted into the quartz tube of our thermal CVD system. Pretreatment was then carried out for 1 h in the flow of hydrogen (270 sccm) and nitrogen (150 sccm) at 800 °C. This process will form Fe nanoparticles (diameter ~20–40 nm) for the growth of MWNTs.

MWNTs were then grown at 800 °C for 2 h by using [Fig. 1(a)] pure C_2H_2, [Fig. 1(b)] C_2H_2 and Ar, [Fig. 1(c)] C_2H_2 and H_2, or [Fig. 1(d)] C_2H_2 and N_2. In all cases, the flow rate of C_2H_2 was fixed at 60 sccm. In this way, the

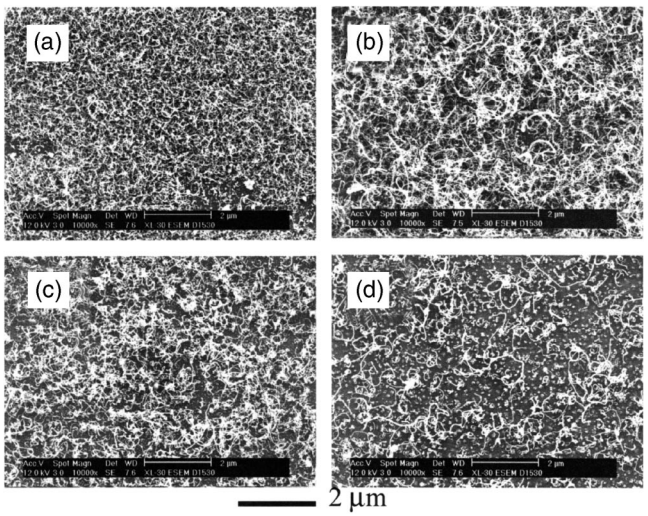

FIG. 1. SEM images of MWNTs grown at 800 °C by using (a) pure C_2H_2, (b) C_2H_2 and Ar, (c) C_2H_2 and H_2, or (d) C_2H_2 and N_2.

[a)]Author to whom corresponding should be addressed; electronic mail: ykyap@mtu.edu

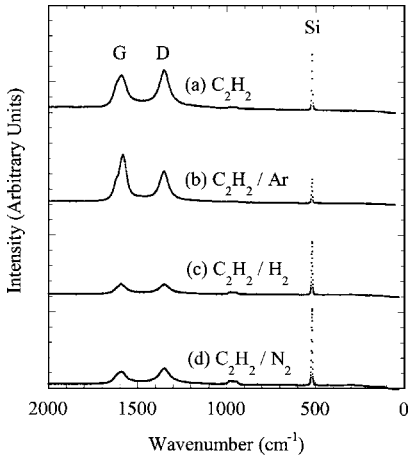

FIG. 2. Raman spectra for MWNTs grown at 800 °C by using (a) pure C_2H_2, (b) C_2H_2 and Ar, (c) C_2H_2 and H_2, or (d) C_2H_2 and N_2.

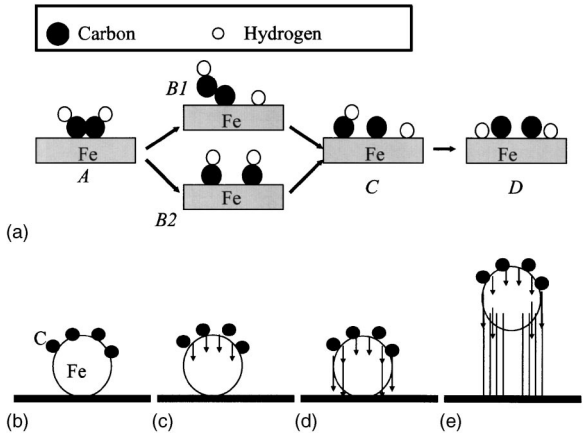

FIG. 3. (a) Sequences of dissociative adsorption of C_2H_2 on Fe surface. The (b) decomposed carbon atoms (c) diffused into the Fe nanoparticle until (d) supersaturation and (e) segregate as nanotubes.

effect of carrier gases (200 sccm for H_2, and 60 sccm for Ar and N_2) on the growth of MWNTs can be determined. After the growth, the CVD system was cooled to room temperature in the flow of the carrier gases [cases (b), (c), and (d)], or Ar gas for case (a). All samples were then examined under scanning electron microscopy (SEM), transmission electron microscopy (TEM), and Raman spectroscopy.

The SEM images of MWNTs grown at these conditions are shown in Fig. 1. These MWNTs have diameters ranging from ~15–30 nm as observed by high-resolution SEM. These are slightly smaller than the diameters of Fe particles observed by AFM. The overall growth morphologies of MWNTs are different when deposited at different gases. The lengths of MWNTs grown by pure C_2H_2 gas [Fig. 1(a)] are typically 2 μm long. The addition of Ar gas [Fig. 1(b)] led to a thicker deposit due to the stacking of individual nanotubes. These MWNTs were significantly longer (estimated as ~10 μm under dynamic SEM imaging) than those grown by pure C_2H_2. The addition of H_2 gas to C_2H_2 [Fig. 1(c)] also increased the length of MWNTs. In addition, the growth of these MWNTs did not occur on all Fe nanoparticles. Bare Fe particles are clearly seen on the substrate. This effect is more obvious for samples grown by C_2H_2/N_2 gas mixture [Fig. 1(d)]. As shown, the growth density is further reduced.

The change of growth density is verified by Raman spectroscopy. In Fig. 2, spectra of these samples are plotted in the same scale. All of these spectra have a strong Si peak at ~520 cm^{-1} coming from the substrates. The nanotubes spectra consist of a graphite peak (G) at ~1590 cm^{-1} and a disorder-induced (D) peak at ~1350 cm^{-1} representing zone center phonons of E_{2g} symmetry and K-point phonons of A_{1g} symmetry, respectively.[12,13] The relative intensity of the G and Si peaks (I_G/I_{Si}) will increase with the increase of nanotubes growth density. Higher growth density will initiate a stronger G peak from the nanotubes and weaker Si signal from the substrate as the excitation laser ($\lambda \sim 514$ nm) beam was partially shielded by the nanotubes. As shown, the I_G/I_{Si} ratios for samples grown by [Fig. 2(a)] pure C_2H_2, and [Fig. 2(b)] C_2H_2/Ar, [Fig. 2(c)] C_2H_2/H_2, and [Fig. 2(d)] C_2H_2/N_2 gas mixtures are 0.62, 1.9, 0.30, and 0.16, respectively. This means, the addition of Ar to C_2H_2 increases the growth density of MWNTs, while the addition of H_2 and N_2 gases decreases the growth density, as is consistent with the SEM images in Fig. 1. We also observed the change of relative intensity between the G and D peaks. These are related to the structural changes of MWNTs as we detected by TEM. The mechanism involved is still under investigation and will be discussed in the future.

We explain the change of growth rate and growth density by referring to dissociative adsorption [Fig. 3(a)] and the VLS growth model [Figs. 3(b) to 3(e)]. As summarized in Fig. 3(a), adsorption of C_2H_2 molecules (step A) will lead to either the breaking up of C—H bond (step B1) to form C_2H and H fragments or C=C bond (step B2) to form two C–H fragments. The function of Fe is reducing the energy required for decomposition by a charge transfer from hydrocarbon molecules to Fe. According to a first principles calculation,[7] the dissociation energy of the first hydrogen atom from an isolated C_2H_2 (steps A to B1) in a vacuum can be reduced from 5.58 eV to 0.96 eV. Likewise, the energy barrier from A to B2 is 1.25 eV. The C–H bond breaking (step B1) is followed by C–C bond breaking (step C) with an energy barrier of 1.02 eV. Whereas, C=C bond breaking (step B2) is followed by C–H bond breaking (step C) with a potential barrier of 0.61 eV. Both modes (A to B1 to C or A to B2 to C) are possible and give one C–H fragment, one C and one H. The decomposition of C_2H_2 is completed after the breaking of the last C–H bond (step D) at a potential barrier of 0.61 eV.

The [Fig. 3(b)] decomposed carbon atoms will then [Fig. 3(c)] diffuse into the Fe nanoparticles. At our growth temperature (800 °C), these nanoparticles are not melted[14,15] even after considering the eutectic point of Fe–C phase[16,17] Since dissociative adsorption is an exothermic process,[5–7] the near-surface temperatures of the nanoparticles will be higher than 800 °C. Further, with the melting of nanoparticles starts from their surfaces,[18] it is possible that the near-surface region will form the gas–liquid interface between carbon and Fe solid-core nanoparticles. Due to the high diffusion rate of carbon in Fe melt, a Fe–C alloy will start to form. When these nanoparticles become [Fig. 3(d)] supersaturated with carbon to a value critical for growth at the solid–liquid interface, the excess carbon will [Fig. 3(e)] segregate as carbon nanotubes in a tip-growth mode (as confirmed by SEM).

Based on these integrated mechanisms, we explain the effect of carrier gas in Fig. 1. In fact, the growth of MWNTs by pure C_2H_2 gas was terminated after ~15 min. Subsequent experiments had shown that the growth patterns of MWNTs from pure C_2H_2 gas for 15 min are similar to those grown for 2 h. We think that our growth condition initiated excessive

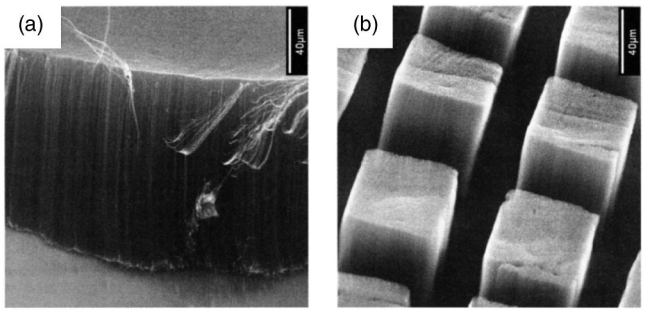

FIG. 4. SEM images of (a) high-density vertically aligned MWNTs grown at 650°C for 15 min by using C_2H_2 and Ar mixed gas. (b) Patterned growth of MWNTs microtowers. Scale bar: 40 μm.

decomposition of C_2H_2 on the surfaces of Fe nanoparticles. This has led to the formation of amorphous carbon on the surfaces of nanoparticles and prevented further contact of C_2H_2 molecules with Fe. Thus, the supply of carbon was terminated. This happened because the decomposition rate of C_2H_2 was higher than the carbon diffusion rate into the Fe nanoparticles, and the segregation rate of carbon from the nanoparticles.

We then examined the growth of MWNTs from the C_2H_2/Ar mixture at periods shorter than 2 h. The growth density of MWNTs increases with the growth duration. MWNTs continued to grow for 2 h in the C_2H_2/Ar mixture. The addition of Ar reduces the density of C_2H_2 molecules on the surfaces of Fe nanoparticles (dilution effect). This has prevented excessive decomposition of C_2H_2 molecules. Thus, the rate of carbon supply and carbon segregation was balanced for continued growth.

The addition of H_2 gas to C_2H_2 introduced two effects. First, the concentration of C_2H_2 is decreased due to dilution. Additional experiments confirmed that MWNTs continued to grow for 2 h. Second, the growth density of MWNTs was reduced since some particles were occupied for the decomposition of H_2 and resulted in insufficient carbon supply for growing MWNTs. H_2 is known to dissociate on the surface of Fe at high temperatures.[5,6] It is possible that C_2H_2 and H_2 molecules are competing for dissociative adsorption on the Fe nanopartcles. Besides, cross interaction between the decomposed hydrogen and hydrocarbon species could result in the removal of carbon deposits (cleaning effect)[19] and thus reduce the growth density.

The addition of N_2 gas to C_2H_2 gas further suppressed the growth density of MWNTs. This could be related to the cross interaction between C_2H_2 and N_2 molecules on the Fe surfaces. It is possible that CN radicals will be formed, which are volatile at high temperatures.[12] This will reduce the carbon flux that diffuse into the Fe nanoparticles and thus reduce the chances of MWNT formation. The actual reason is subjected to further investigations. The diluting effect of N_2 gas is similar to those in Ar and H_2 gases and results in longer tubes in 2 h.

From these results, we understood that it is important to balance the decomposition rate of C_2H_2 and the segregation rate of carbon. We then optimize the growth of MWNTs by C_2H_2/Ar gas mixture by simply varying the growth temperatures. At 650°C, we were able to grow high-density MWNTs as shown in Fig. 4(a) at a tilted angle of 40° from the aerial view. As shown, these MWNTs are vertically aligned due to the van der Waals forces between adjacent MWNTs, which restrict the growth toward the free space (vertically upward). We think that this efficient growth process occurs at partial pressures and temperature at which the decomposition and segregation rates of carbon are balanced. As compared to the case shown in Fig. 1(b), this aligned growth is due to a lower growth temperature, which reduced the decomposition rate of C_2H_2 molecules and suppressed the formation of amorphous carbon films on some Fe catalysts. This could have further increased the growth density and thus resulted in aligned growth. These MWNTs can also be grown to desired patterns, for instance, MWNTs microtowers shown in Fig. 4(b). All these samples were grown for 15 min with an estimated length of $\sim$200 μm: A remarkable growth rate of $\sim$800 μm/h. However, our experiments show that this growth rate is decreasing with time. This means, other factors that affect the growth rate have occurred and are subjected to further investigation.

In summary, the addition of carrier gas can suppress the decomposition rate of C_2H_2 by diluting the density of C_2H_2 on the Fe catalyst surface. This will increase the growth rate of MWNTs that was initially saturated. In addition, both H_2 and N_2 can reduce the growth density of MWNTs and thus can be used for density control. A balance between the carbon supply (decomposition) and segregation rates is required for high-density and high growth rate of MWNTs. These results could facilitate continued growth of carbon nanotubes in the future by *in situ* control of the dissociative adsorption of hydrocarbon molecules on catalyst surfaces.

One of the authors (Y.K.Y.) acknowledges support from the Michigan Tech Research Excellence Fund and the Army Research Office (W911NF-04-1-0029, through the City College of New York). Two of the authors (S.D. and Y.G.) were supported by DOE Grant No. BSE-DE-FJ02-01ER45932.

[1] S. Iijima, Nature (London) **354**, 56 (1991).
[2] *Carbon Nanotubes: Synthesis, Structure, Properties, and Applications*, edited by M. S. Dresselhaus and G. Dresselhaus, (Springer, Berlin, 2001).
[3] G. W. Wagner and W. C. Ellis, Appl. Phys. Lett. **4**, 89 (1964).
[4] E. I. Givargizov, in *Current Topics In Materials Science*, edited by E. Kaldis (North–Holland, Amsterdam 1978), Vol. I, Chap. 3.
[5] W. Morits, R. Imbihi, R. J. Behm, G. Ertl, and T. Matsushima, J. Chem. Phys. **83**, 1959 (1985).
[6] P. Jiang, M. Zappone, and S. L. Bernasek, J. Chem. Phys. **99**, 8126 (1993).
[7] G.-D. Lee, S. Han, J. Yu, and J. Ihm, Phys. Rev. B **66**, 081403(R) (2002).
[8] D. B. Geohegan, A. A. Puretzky, I. N. Ivanov, S. Jesse, G. Eres, and J. Y. Howe, Appl. Phys. Lett. **83**, 1851 (2003).
[9] G. Eres, A. A. Puretzky, D. B. Geohegan, and H. Cui, Appl. Phys. Lett. **84**, 1759 (2004).
[10] C. J. Lee and J. Park, Appl. Phys. Lett. **77**, 3397 (2000).
[11] T. Kim, K. R. Lee, K. Y. Eun, and K. H. Oh, Chem. Phys. Lett. **372**, 603 (2003).
[12] Y. K. Yap, S. Kida, T. Aoyama, Y. Mori, and T. Sasaki, Appl. Phys. Lett. **73**, 915 (1998).
[13] Y. K. Yap, M. Yoshimura, Y. Mori, and T. Sasaki, Appl. Phys. Lett. **80**, 2559 (2002).
[14] P. Buffat and J.-P. Borel, Phys. Rev. A **13**, 2287 (1976).
[15] A. Moisala, A. G. Nasibulin, and E. I. Kauppinen, J. Phys.: Condens. Matter **15**, S3011 (2003).
[16] O. Kubaschewski, *Iron-binary Phase Diagram* (Springer, Berlin, 1982).
[17] B. Chicco and W. R. Thorpe, Metall. Trans. A **A3**, 1293 (1982).
[18] Z. L. Wang, J. M. Petroski, T. C. Green, and M. A. El-Sayed, J. Phys. Chem. B **102**, 6145 (1998).
[19] G. A. Jablonski, F. W. A. H. Geurts, and A. Sacco, Jr., Carbon **30**, 99 (1992).